Japanese Journal of Applied Physics **50** (2011) 052101 **REGULAR PAPER**
DOI: 10.1143/JJAP.50.052101

N-Polar III–Nitride Green (540 nm) Light Emitting Diode

Fatih Akyol[1]*, Digbijoy N. Nath[1], Emre Gür[1,2], Pil Sung Park[1], and Siddharth Rajan[1]

[1] *Department of Electrical and Computer Engineering, The Ohio State University, Columbus, OH 43210 U.S.A.*
[2] *Department of Physics, Faculty of Science, Atatürk University, 25240 Erzurum, Turkey*

Received October 1, 2010; accepted February 23, 2011; published online May 20, 2011

We report the demonstration of a N-polar InGaN based green light emitting diode (LED) grown by N_2 plasma-assisted molecular beam epitaxy (PAMBE). High quality multiple quantum well LEDs with $In_{0.29}Ga_{0.71}N$ quantum wells were grown at a temperature of 600 °C by applying a new growth model. LED structures exhibited green emission, and electroluminescence measurements on the test structure showed peak emission wavelengths varying from 564.5 to 540 nm. The full width at half-maximum reduced from 74 to 63 nm as the drive current was increased to 180 A/cm^2. This work is the first demonstration of an N-polar LED with emission in the green wavelength range.
© 2011 The Japan Society of Applied Physics

1. Introduction

InGaN-based laser diodes (LD) and light emitting diodes (LED) emitting in the UV and blue wavelength range have found wide applications in optical storage and lighting applications.[1,2] There have been many studies on various planes of nitride crystals to obtain LEDs and LDs operating at longer wavelengths with high efficiencies.[3,4] More than 50% external quantum efficiencies (EQE) have been achieved for blue LEDs with both *c*-plane and semi-polar orientations whereas the maximum EQE ever reported for a green LED is 30%.[4] One of the main reasons for decreasing efficiency for longer wavelengths is that emitters for green and longer wavelengths still pose significant growth and device design challenges.[5] Firstly, due to the higher volatility of In species, higher In content InGaN requires lower growth temperatures than the optimal growth temperature of GaN. This mismatch in optimal growth temperatures leads to challenges in the growth of high quality InGaN/GaN multiple quantum well (MQW) emitters. Secondly, polarization effects are more pronounced as the In composition is increased, It is expected that the relatively high polarization fields in *c*-plane oriented InGaN/GaN emitters could lead to poor carrier confinement and consequently poor efficiency in LED structures.

The N-polar orientation of GaN has several advantages that make it attractive for high In composition InGaN growth. N-polar InN can be grown by plasma-assisted molecular beam epitaxy PAMBE at higher temperatures (approximately 100 °C higher) than In-polar InN,[6,7] This is attributed to the higher stability of InN on the N-polar surface. Recent work on N-polar InGaN growth demonstrated significantly higher growth temperatures and In incorporation on N-polar InGaN when compared to Ga-polar InGaN.[8] The direction of the spontaneous and piezoelectric polarization in N-polar is reversed from that of Ga-polar, which may provide advantages for LED operations. In addition, polarization plays a critical role in device operation of all polar emitters, and investigation of N-polar InGaN-based heterostructure devices provides a route to investigate these effects. Since the polarization field increases with In composition, these effects are more pronounced as longer emission wavelengths are targeted. Although N-polar electronic devices with performance comparable to Ga-polar ones have been reported,[9]

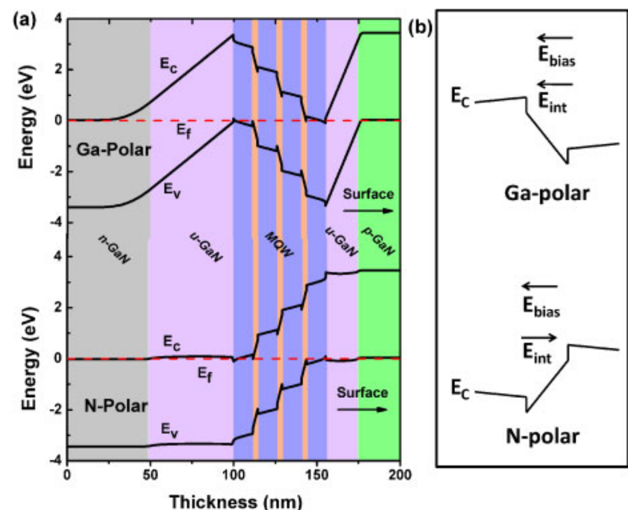

Fig. 1. (Color online) (a) Computed energy band diagrams of a typical InGaN MQW device with both polarities. (b) State of the intrinsic (including both spontaneous and piezoelectric polarization) and bias induced electric fields in the QWs of a typical device in both polarities.

there are relatively fewer reports on N-polar InGaN growth for optoelectronic applications,[10–12] In this letter, we report on the growth and optical characterization of N-polar InGaN based MQW LED grown by PAMBE.

In Fig. 1(a), equilibrium energy band diagrams of N- and Ga-polar typical InGaN/GaN MQW heterostructures are shown. The energy band diagrams were calculated using a self-consistent Schrödinger–Poisson solver that incorporates spontaneous and piezoelectric polarization.[13] In the Ga-polar LED structure, the polarization fields are reversed with respect to the p–n junction depletion field, thus leading to a wider depletion region, However, in the case of the N-polar structure, the polarization acts in the same direction as the depletion, and the depletion region is therefore reduced. This is expected to lead to a lower turn-on voltage for the N-polar p–n junction. It can be seen from Fig. 1(b) that due to the reverse direction of polarization in a N-polar device, an increase in forward bias voltage assists the field in QW regions to approach flat-band conditions leading to suffering less from stark effect across the QW. However, in a Ga-polar device structure, increasing forward bias voltage increases the field in the QWs, thus decreasing the electron and hole wave-function overlap in the quantum wells. The direction

*E-mail address: akyolf@ece.osu.edu

 © 2011 The Japan Society of Applied Physics

of polarization in N-polar GaN therefore seems more favorable to LED operation than in the case of Ga-polar GaN. It is also observed from the same figure that the injected carriers come across a potential barrier for Ga-polar structure which decreases the carrier injection efficiency and shows itself as higher turn-on voltages. Conversely, in the reversed polarization the potential barrier against the injection is eliminated which is obviously favorable to obtain lower turn-on voltages.

2. Experimental Procedure

The sample used in this study was grown on N-polar free standing LED quality GaN template (dislocation density $\sim 10^8\,\text{cm}^{-2}$) obtained from Lumilog by rf-plasma assisted molecular beam epitaxy in a Veeco Gen 930 system equipped with standard Knudsen cells for Ga and In.[14] Active nitrogen was supplied using a Veeco RF plasma source. Following the growth model for N-polar InGaN growth by PAMBE,[8] a Ga-flux was chosen to achieve 29% In mole fraction at a growth temperature of 600 °C. The growth of the active MQW region was performed in an N_2-limited and In rich growth regime with excess In coverage on the surface. The nominal growth rate defined by the N_2-stoichiometric flux in the absence of InGaN decomposition is 5 nm/min. However as predicted by the growth model, for the In composition and growth temperature used for this growth, a reduced growth rate of 3.25 nm/min was calculated accounting for decomposition to grow 3 nm of $In_{0.29}Ga_{0.71}N$ QW and 12 nm $In_{0.14}Ga_{0.86}N$ barrier, the compositions being verified by X-ray diffraction (XRD) scan data with simulation (inset of Fig. 2). The growth of InGaN QW and a GaN (or InGaN) barrier without growth interruption with a single Ga effusion cell in PAMBE poses severe challenges because the growth temperature as well as the Ga flux required for the growth of QW and barrier is significantly different. An N_2-pulsing scheme was hence employed to grow the barrier where In and Ga shutters were kept open throughout with the Ga-flux at the same value as used for preceding quantum well layer growth. The duty cycle of the pulse was adjusted to get InGaN with a higher Ga mole fraction. To investigate the surface morphology of the QW layer, a test sample was grown in identical conditions with the growth intentionally terminated with a $\sim$2 nm $In_{0.05}Ga_{0.95}N$ (to prevent decomposition) on a single 3 nm $In_{0.29}Ga_{0.71}N$ QW layer. The atomic force microscopy (AFM) image shows smooth surface morphology (inset to Fig. 2: $2 \times 2\,\mu\text{m}^2$ scan).

LEDs were fabricated using conventional optical lithography. Ni/Au/Ni (5/5/1 nm) metal stack was evaporated to form the p-type electrode. Following the p contact evaporation, mesa isolation of the devices was performed by Cl-based inductively coupled plasma (ICP) etching with $Cl_2/BCl_3/Ar$ (50/5/5 sccm) plasma under 40 W ICP power and 3 W RF power for 30 min. Finally, Ti/Au (20/100 nm) n-contact was deposited on the etched n-GaN layer. All measurements reported were performed on a 17,000 μm^2 device at room temperature under continuous wave operation.

3. Results and Discussion

Current–voltage (I–V) characteristics of a typical N-polar LED are shown in the inset of Fig. 3. The differential

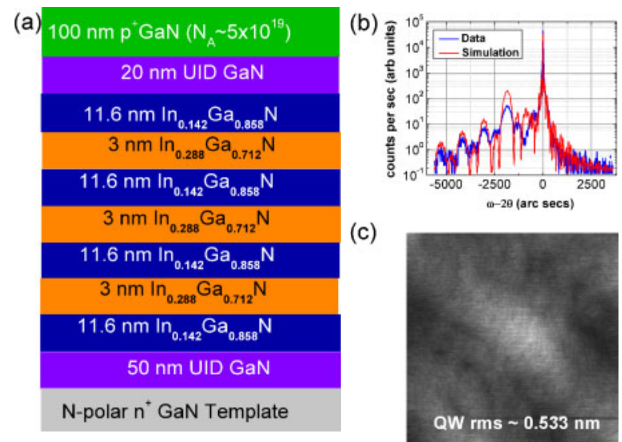

Fig. 2. (Color online) (a) The epitaxial design of the MQW green LED, (b) ω–2θ XRD curves of the sample, and (c) AFM image of the sample showing the surface morphology of the quantum-well/barrier layer.

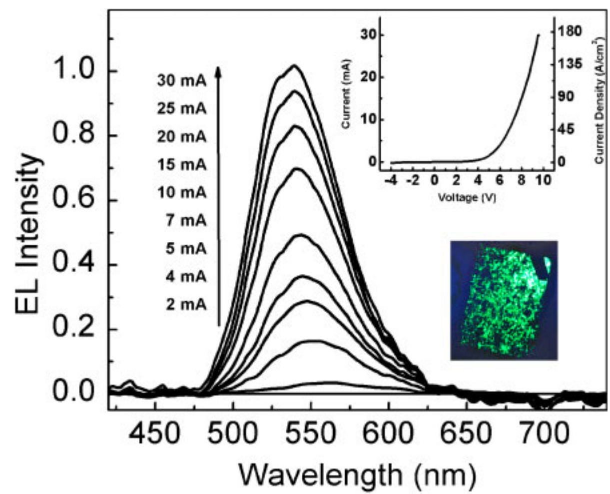

Fig. 3. (Color online) EL spectra as a function of DC driving currents varying from 2 to 30-mA (11 to 176 A/cm^2). The above inset shows the I–V characteristics of the 17,000 μm^2 LED and the bottom one shows the image of the forward biased LED.

resistance and turn-on voltage were 0.012 $\Omega\cdot\text{cm}^2$ (72 Ω) and 5 V, respectively. The image of the forward biased LED is shown in the inset of Fig. 3. We attribute the light intensity variation observed across the contact to unoptimized ohmic contacts and growth of p-GaN layer. The electroluminescence (EL) spectra for increasing driving current are shown in Fig. 3. The maximum current driven in this regime was 30 mA, corresponding to a density of 176 A/cm^2. The peak wavelengths, peak intensities and full width at half maximum (FWHM) as a function of driving current are shown in Fig. 4. An increase in the driving current results in a linear increase in the EL emission intensity up to 88 A/cm^2, and after that point, it starts to saturate depending on the increasing heating effect on the device operation. The peak wavelengths were measured as 563 and 540 nm at 2 and 30 mA, respectively. The 23 nm blue shift over 28 mA (165 A/cm^2) is attributed to screening of the piezoelectric field by electrons and holes at higher injection current density.[15] Note that there is only 0.7 nm blue shift from 88

 © 2011 The Japan Society of Applied Physics

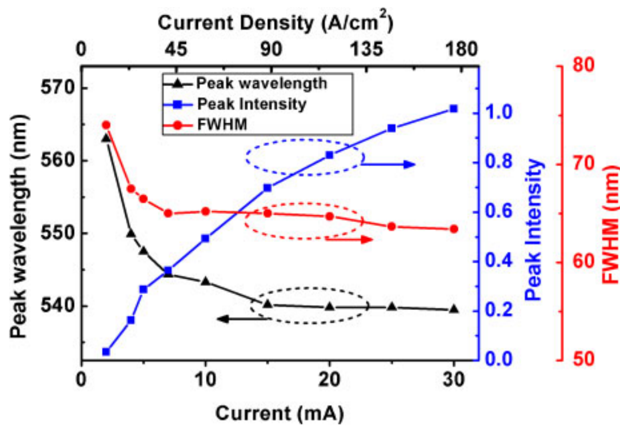

Fig. 4. (Color online) EL emission peak intensities (normalized to the highest value), peak wavelengths and FWHMs as a function of driving current from 2 to 30 mA (11 to 176 A/cm^2).

to 176 A/cm^2 which may result from a competition between state-filling effect and heat generation.[16] The FWHM variation as a function of driven current showed a fast decreasing trend from 74 to 65 nm up to a current density of 45 A/cm^2 then, it slowly decreases to a value ~63.4 nm for the rest of the current density regime. Based on the previous reports, it can be observed that FWHM decreases as current increases at low current density regimes ($\lesssim$25 A/cm^2) and increases at higher current densities.[16]

We note that the measured FWHM is higher than that observed in the state-of-art green LEDs grown, for example, by metal organic chemical vapor deposition (MOCVD).[16,17] The growth conditions used for the LEDs described in this work were optimized only to achieve the required emission wavelength. The FWHM is mostly dependent on the microscale compositional and thickness uniformity of the InGaN wells, which in turn are greatly dependent on the growth parameters such as temperature, flux, etc. We have not carried out growth optimization to minimize the FWHM, and it is likely that the fluctuations in Indium and quantum well thickness contribute to the FWHM. Further investigation in this direction should lead to lower FWHM, and better emission results.

The decrease of FWHM at low current density has been attributed to band filling effects caused by potential fluctuations, while the increase at higher current density is due to screening charges and excess heat generation.[16,18,19] The behavior of N-polar LED in the present study might be attributed to the dominating effect of In fluctuations due to the unoptimized growth conditions which also results in greater than expected FWHM values for this wavelength range. While further investigations are needed to clarify these issues, the FWHM saturation at high current regimes might result from a competition between band filling effect and excess heat generation which can be seen as a deviation from linearity of the peak intensity variation with current density (Fig. 4).

4. Conclusions

In conclusion, an MBE grown N-face InGaN green LED was realized and fabricated successfully. The EL measurement results of the device showed a short blue shift from 563 to 540 nm and a decreasing FWHM from 74 to 63.4 nm under 165 A/cm^2 current range. Our results show that the EL FWHM values are high and saturate at high current range. We speculate that this behavior may result from unoptimized growth conditions which cause higher In fluctuations. This demonstration of green emission by MBE grown N-polar InGaN-based LEDs could lead to improved understanding of polarization effects on LED performance.

Acknowledgements

We would like to acknowledge funding from ONR (Paul Maki, Program Manager) and OSU Institute for Materials Research (IMR). Dr. Emre Gür would like to thank for the support to the Scientific and Technological Research Council of Turkey (TUBITAK) 2219 project program. Also, we want to thank to Mr. V. Protasenko for his help to do EL measurements.

1) S. Nakamura, M. Senoh, S. Nagahama, N. Iwasa, T. Yamada, T. Matsushita, H. Kiyoku, and Y. Sugimoto: Jpn. J. Appl. Phys. **35** (1996) L74.
2) S. Nakamura, M. Senon, and T. Mukai: Jpn. J. Appl. Phys. **32** (1993) L8.
3) T. Detchprohm, M. Zhu, Y. Li, L. Zhao, S. You, C. Wetzel, E. A. Preble, T. Paskova, and D. Hanser: Appl. Phys. Lett. **96** (2010) 051101.
4) Y. Zhao, J. Sonoda, C. Pan, S. Brinkley, I. Koslow, K. Fujito, H. Ohta, S. P. DenBaars, and S. Nakamura: Appl. Phys. Express **3** (2010) 102101.
5) R. Stevenson: IEEE Spectrum **47** [3] (2010) 34.
6) K. Xu and A. Yoshikawa: Appl. Phys. Lett. **83** (2003) 251.
7) H. Naoi, F. Matsuda, T. Araki, A. Suzuki, and Y. Nanishi: J. Cryst. Growth **269** (2004) 155.
8) D. Nath, E. Gur, S. Ringel, and S. Rajan: Appl. Phys. Lett. **97** (2010) 071903.
9) S. Rajan, A. Chini, M. H. Wong, J. S. Speck, and U. K. Mishra: J. Appl. Phys. **102** (2007) 044501.
10) J. Abell: Dr. Thesis, Collage of Engineering, Boston University, Boston, MA (2008).
11) X. Q. Shen, T. Ide, M. Shimizu, and H. Okumura: J. Cryst. Growth **237–239** (2002) 1148.
12) H. Masui, S. Keller, N. Fellows, N. A. Fichtenbaum, M. Furukawa, S. Nakamura, U. K. Mishra, and S. P. DenBaars: Jpn. J. Appl. Phys. **48** (2009) 071003.
13) M. Grundmann: BandEng [http://www.michaelgrundmann.com].
14) Lumilog: www.lumilog.com
15) P. Perlin, C. Kisielowski, V. Iota, B. A. Weinstein, L. Mattos, N. A. Shaprio, J. Kruger, E. R. Weber, and J. Yang: Appl. Phys. Lett. **73** (1998) 2778.
16) M. Funato, M. Ueda, Y. Kawakami, Y. Narukawa, T. Kosugi, M. Takahashi, and T. Mukai: Jpn. J. Appl. Phys. **45** (2006) 659.
17) Y. Lin, A. Chakraborty, S. Brinkley, H. C. Kuo, T. Melo, K. Fujito, J. S. Speck, S. P. DenBaars, and S. Nakamura: Appl. Phys. Lett. **94** (2009) 261108.
18) Y. D. Qi, H. Liang, D. Wang, Z. D. Lu, W. Tang, and K. M. Lau: Appl. Phys. Lett. **86** (2005) 101903.
19) S. Yamamoto, Y. Zhao, C. Pan, R. B. Chung, K. Fujito, J. Sonoda, S. P. DenBaars, and S. Nakamura: Appl. Phys. Express **3** (2010) 122102.

 © 2011 The Japan Society of Applied Physics